

## DYNAMIC BEHAVIOR OF FLOOR SLAB WITH STIFFENER BEAM DUE TO BLAST LOAD FROM MODIFICATION OF REED EQUATION

Haryo Koco Buwono<sup>1</sup>

<sup>1</sup>Civil Engineering Study Program, University of Muhammadiyah Jakarta, Jl. Cempaka Putih Tengah 27, Jakarta

Correspondence email: haryo.koco@umj.ac.id

Received December 8, 2020 | Accepted January 29, 2021

### ABSTRACT

Explosions in buildings are not always the result of terrorist attacks, but can also be caused by several work accidents due to explosive tools or materials as trigger of problems in construction. Friedlander's equation has many modifications including the Reed equation. Reed proposes a modification of Friedlander equation using 4th order polynomial. The Reed equation is still not close relatively to the Friedlander equation. The Reed equation is only calculated up to  $t = 25/7$  (s) in the negative phase. Meanwhile, the Friedlander is calculated at  $t = 5$  if both are reviewed at no load or one unit condition. It is necessary to evaluate using the 4th order polynomial equation which is close to the Friedlander explosion equation. Dynamic behavior of structures must be considered in the design of structural elements. The purpose of this study is to analyze numerically the effect of explosions on orthotropic slabs which have partial fixity placement and stiffeners in the  $x$  direction, namely in the short span direction. The behavior of the plate orthotropic configuration, the localized blast load are centered in the middle of the strain, and the effect of thickness and stiffening on the vertical deflection of the plates are solved numerically using two auxiliary equations in the  $x$  and  $y$ -directions. From the analysis, it is found that there is vertical deflection with related to time. This paper introduces the dynamic behavior of Reed's modified blast loads with 4th order polynomial on orthotropic plates with  $x$ -direction stiffener beam.

**Keywords:** blast loads, slabs, stiffeners, Reed, 4th order polynomials

## 1. INTRODUCTION

### Background

The floor slab system chosen for building is different, depending on the function of the space and economic limitations and architectural requirements. The reinforced concrete slab system in the SNI 2847: 2019 regulation consists of two, namely one way slab (one-way plate) and two way slab (two-way plate) (SNI 03-2847:2019, 2019). The plate design in the ideal plan is to be able and effective to withstand any loads that may work on the plate, including

explosion loads. An explosion is a very fast chemical reaction releasing pressure and heat energy that only lasts a few milliseconds. The resulting pressure is enormous through the air and fills the entire space through propagating waves that are faster than the speed of sound. The enormous pressure of the explosion presses the air around the explosion, creating the effect of the blast wave (Rigby et al., 2014). Each explosion wave is characterized by the following parameters: (a) positive ( $P_{so}$ ) and negative pressure

peaks, (b) the explosion period is positive ( $t_{dp}$ ) and negative ( $t_{dn}$ ) duration. The explosion load scenario is influenced by the equation model which is inputted as a dynamic load in the construction (Karlos & Solomon, 2013). The Reed's equation in 1977 states that the Friedlander's equation in 1946 uses blast load equation approach as follow: (1)

$$p_r(t) = p_{r,max} \left(1 - \frac{t}{t_d}\right) e^{-bt/td} \quad (1)$$

According to Smyth theory, an approach to the convenience of using polynomial equation (Smyth, 2014), which is stated as follows. (Garces, 2019).

$$P(t) = P_r \left(1 - \frac{t}{td}\right) \left[1 - \frac{7t}{25td}\right] \left[1 - \left(\frac{7t}{25td}\right)^2\right], \quad 0 \leq t \leq \frac{25}{7} \quad (2)$$

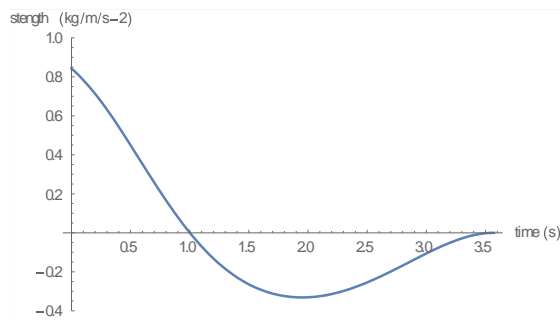


Figure 1. Reed's Blast Load Equation in 1977 (Garces, 2019)

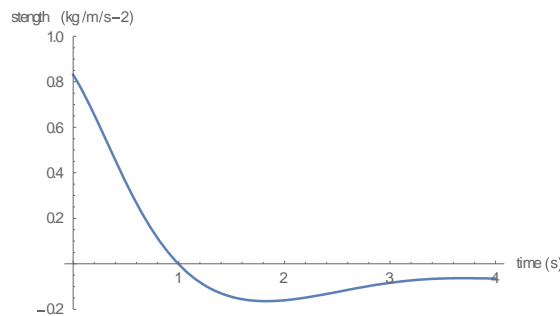


Figure 2. Polynomial Blast Load Equation of 4<sup>th</sup> Order (Buwono et al., 2020)

In Figure 1, Reed's polynomial equation states that the  $t_d$  limit (positive phase duration) is to solve the entire positive phase and the negative phase of the explosion at once. After the blast load passes through its positive phase, the load behavior changes to a negative pressure load (suction) (Bryant et al., 2013). This phase generally has a maximum amplitude less than the positive phase, but a longer

duration, roughly twice the duration of the positive phase. After going through these two phases, the explosion has an advanced phase, namely the free vibration phase, or the no-load phase. The plates are more affected by the impact after explosion or on the free vibration phase (Ahmet Tuğrul & Sevim, 2017).

### Polynomial of 4<sup>th</sup> Order on Reed's Approach

Figure 2 is Reed modification explosion phase using 4<sup>th</sup> order polynomial. That approach uses the regression method based on the smallest error factor, which the equation is as follows:

$$P(t) = P_r \left(0,0151 \left(\frac{t}{td}\right)^4 - 0,1946 \left(\frac{t}{td}\right)^3 + 0,8949 \left(\frac{t}{td}\right)^2 - 1,6898 \left(\frac{t}{td}\right) + 0,9720\right);$$

$$0 \leq t \leq td \quad (3)$$

The equation (3) to the equation (1) has an error factor of 1.64%. Meanwhile, the Reed equation in 1977 has an error of 8.96%. Based on Figure 1, the error factor for Reed's equation turns out to have a large error for Friedlander in 1946, which is 7.33%. Viewing from the approach or modification of the Friedlander explosion equation, the polynomial equation is closer to the actual Friedlander equation in 1946. In this paper, furthermore using the 4<sup>th</sup> order polynomial (Buwono et al., 2020).

### Floor Slab Description

In analyzing a structure, it is necessary to know how the structure behaves to various kinds of excitation or vibration. One of the quantities that reflect the behavior of a structure is its natural frequency. The natural frequency of the structure can be found by assuming that the structure has no damping and no loading acts on the structure, only initial conditions. This is also commonly known as free vibration analysis.

The damped elastic orthotropic plate differential equation is obtained by adding up all the internal forces acting on the plate system which must be balanced with the acting external loads.

$$D_x \left( \frac{\partial^4 w(x,y,t)}{\partial x^4} \right) + 2B \left( \frac{\partial^4 w(x,y,t)}{\partial x^2 \partial y^2} \right) + D_y \left( \frac{\partial^4 w(x,y,t)}{\partial y^4} \right) + \xi h \left( \frac{\partial w(x,y,t)}{\partial t} \right) + \rho h \left( \frac{\partial^2 w(x,y,t)}{\partial t^2} \right) = p_z(x,y,t) \quad (4)$$

For rectangular orthotropic plates rigid with stiffener beam, the equation (4) can be used to obtain the response of the plates to a particular load. The geometric parameters that need to be known on a rectangular orthotropic plate that is rigid with joists can be seen in Figure 3.

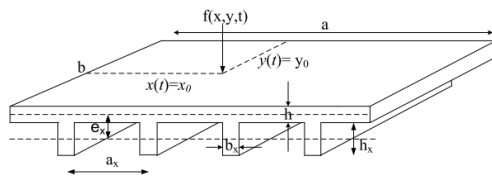


Figure 3. Rectangular Orthotropic Plate with Stiffener Beam

### Levy's Solution

To solve the equation of motion above, the first is to use the boundary conditions of the joint on all four sides. This condition will occur angular rotation on the edge of the plate but there will be no bending moment. Simple leaning conditions can be solved with Navier's solution or Levy solution. Finding a solution to the equation of motion for the joint condition begins with selecting a trial function that satisfies the boundary conditions of the simple dependent conditions. In this solution, the damping effect on the structure is also neglected (Pevzner et al., 2000).

The chosen trial function equation is the multiplication of two components, namely the spatial function or position and the time function. The transverse deflection of the plates as a function of position and time can be expressed as in the equation (5).

$$w_{(x,y,t)} = w_{(x,y)} t(t) = w_{(x,y)} \sin \omega t \quad (5)$$

Information:

$W_{(x,y)}$  : Position function or spatial Function

$\omega$  : Natural frequency of the system

The trial function equation is substituted into the differential equation of motion for the ortrotopic plate system and algebraic

operations are performed to obtain equation (6) below.

$$\omega_{mn}^2 = \frac{\pi^4}{\rho h} \left[ D_x \left( \frac{m}{a} \right)^4 + 2B \left( \frac{mn}{ab} \right)^2 + D_y \left( \frac{n}{b} \right)^4 \right] \quad (6)$$

Equation (6) is an equation for the eigenvalue for a variety of structures. By calculating the positive root of the eigenvalue, the natural frequency of the structure can be obtained. The equation for obtaining the eigenvalue above only applies to structures with simple boundary conditions on all sides, while the object of this study is a plate structure with partial fixity boundary conditions so that the equation needs to be modified.

### Modified Bolotin Method

Modified Bolotin Method is one way to solve the plate differential equation with partial fixity boundary conditions and can also take into account the effect of high mode.

The eigenvalue for a rectangular plate with partial fixity on all sides can be found by analogizing the plate as a simple rest on all sides. The integer index value for x direction and y direction is replaced by the p coefficient for x and q direction for y direction. The values of p and q are the real numbers obtained looking for a solution to the auxiliary problem. The eigenvalue equation for the plate with the partial fixity boundary condition is expressed as equation (7) below.

$$\omega_{pq}^2 = \frac{\pi^4}{\rho h} \left[ D_x \left( \frac{p}{a} \right)^4 + 2B \left( \frac{pq}{ab} \right)^2 + D_y \left( \frac{q}{b} \right)^4 \right] \quad (7)$$

Information:

p : The real numbers obtained from the auxiliary solution in the x direction

q : The real numbers obtained from the auxiliary solution in the y direction

### First Auxiliary Solution

The trial function for the first spatial auxiliary solution (x direction) is stated as follows:

$$w_{(x,y)} = X_{(x)} \sin \left[ \frac{q\pi y}{b} \right] \quad (8)$$

The equation for the solution of the position function for the x direction is as follows:

$$X(x) = A_1 e^{i\frac{\mu\pi}{a}x} + A_2 e^{-i\frac{\mu\pi}{a}x} + A_3 e^{i\frac{\mu\pi}{a}x} + A_4 e^{-i\frac{\mu\pi}{a}x} \quad (9)$$

So,

$$X(x) = \text{Cosh}\left[\frac{\beta\pi x}{ab}\right] + \frac{(b(pk_1(c_1-c_2)+a(F_1+F_2)s_2))}{(k_1(bp s_1-\beta s_1))} \text{sinh}\left[\frac{\beta\pi x}{ab}\right] - \text{Cos}\left[\frac{\mu\pi x}{a}\right] \quad (10)$$

### Second Auxiliary Solution

The solution of second auxiliary problem can be calculated in the same way as the first auxiliary problem, but the difference is in the second auxiliary is calculated only on the y-axis. The trial function for the second spatial auxiliary solution (y direction) is stated as follows:

$$w_{(x,y)} = Y_{(y)} \sin\left[\frac{p\pi y}{a}\right] \quad (11)$$

The equation for the solution of the position function for the Y direction is as follows:

$$Y(y) = B_1 e^{\frac{\pi}{ab}y} + B_2 e^{-\frac{\pi}{ab}y} + B_3 e^{i\frac{q\pi}{b}y} + B_4 e^{-i\frac{q\pi}{b}y} \quad (12)$$

So,

$$Y = \text{Cosh}\left[\frac{\theta\pi y}{ab}\right] + \frac{(a(qk_2(c_2-c_1)+b(F_3+F_4)s_2))}{(k_2(aq s_2-\theta s_2))} \text{sinh}\left[\frac{\theta\pi y}{ab}\right] - \text{Cos}\left[\frac{q\pi y}{b}\right] + \frac{(ab(F_3+F_4)s_2+\theta k_2(c_2-c_1))}{(k_2(\theta s_2-aq s_2))} \text{sin}\left[\frac{q\pi y}{b}\right] \quad (13)$$

### Total Solution of Plate Motion Equation

The response of the plate to dynamic transverse loads includes two solutions, namely the homogeneous solution (free vibration) and the particular solution (forced vibration). The homogeneous solution and the particular solution are solved separately and the two solutions add up to get the total plate response. That connection can be expressed as the following equation:

$$w_H + w_p = w_{(mnt)} \quad (14)$$

A homogeneous solution,  $w_H$ , is a solution for a structural state that does not accept excitation in the form of a load but a solution that occurs because of the deformation or initial condition that causes a structural response to occur.

The homogeneous solution of the differential equation above is linear so that it can use the superposition method for each auxiliary value of p and q (Shahsavari

& Tofighi, 2014). Therefore, the total homogeneous solution for a given number of modes can be expressed as follows:

$$w_H = w(x, y, t) = \sum_{p=1}^{\infty} \sum_{q=1}^{\infty} W_{pq}(x, y) \cdot T_{pq}(t) \\ = \sum_{p=1}^{\infty} \sum_{q=1}^{\infty} X_{pq}(x) Y_{pq}(y) e^{-\xi \omega_{pq} t} (a_0 \cos(\omega_D t) + b_0 \sin(\omega_D t)) \quad (15)$$

As with the completion of the homogeneous solutions, solving particular solutions also uses the variable separation method. Homogeneous solutions,  $\bar{T}_{pq}(t)$ , still contain constants that can be obtained using the initial conditions. This function shows transient vibration conditions at no load, whereas the particular solution describes the vibrational state. Particular solutions of differential equation,  $T_{pq}^*(t)$ , is a combination of spatial solutions and temporal particular solutions as follows:

$$w_p = \sum_{p=1}^{\infty} \sum_{q=1}^{\infty} X_{pq}(x) Y_{pq}(y) \int_0^t \int_0^a \int_0^b \frac{p(x, y, \tau)}{\rho h Q_{pq}} X_{pq}(x) dx \int_0^b Y_{mn}(y) dy \frac{e^{-\xi \omega_{pq}(t-\tau)}}{\omega_D} \sin(\omega_D(t-\tau)) d\tau \quad (16)$$

The total solution is the real total response which takes into account the effects of both free and forced vibrations. The total solution is obtained by adding the homogeneous solution of equation (15) and the particular solution of equation (16) in order to obtain the following equation:

$$w = \sum_{p=1}^{\infty} \sum_{q=1}^{\infty} X_{pq}(x) Y_{pq}(y) e^{-\xi \omega_{pq} t} (a_0 \cos(\omega_D t) + b_0 \sin(\omega_D t)) \\ + \sum_{p=1}^{\infty} \sum_{q=1}^{\infty} X_{pq}(x) Y_{pq}(y) \int_0^t \int_0^a \int_0^b \frac{p(x, y, \tau)}{\rho h Q_{pq}} X_{pq}(x) dx \int_0^b Y_{mn}(y) dy \frac{e^{-\xi \omega_{pq}(t-\tau)}}{\omega_D} \sin(\omega_D(t-\tau)) d\tau \quad (17)$$

### Moment

A plate with a partial fixity limit on the sides will have a bending moment on the sides, the bending moment value depends on the rotational stiffness on these sides. The boundary conditions for partial fixity conditions are obtained by equations (18) and (19) (Shabana, 2014).

$$M_x(x, y) = -D_x \left( \frac{\partial^2 w(x, y)}{\partial x^2} + \nu_y \frac{\partial^2 w(x, y)}{\partial y^2} \right) = k_1 \frac{\partial w(x, y)}{\partial x} \quad \text{di } x = 0 \text{ dan } x = a \quad (18)$$

$$M_y(x, y) = -D_y \left( \frac{\partial^2 w(x, y)}{\partial y^2} + \nu_x \frac{\partial^2 w(x, y)}{\partial x^2} \right) = k_2 \frac{\partial w(x, y)}{\partial y} \quad \text{di } y = 0 \text{ dan } y = b \quad (19)$$

### Main Stress of Bending Moment

The maximum principal stress is the maximum normal stress when the

orientation of the particles is changed so that the shear stress value is zero. Meanwhile, the minimum main stress is the minimum normal stress when the particle orientation is changed so that the shear stress value is zero. The maximum and minimum principal stresses are calculated by the equation obtained by Mohr's theory (Ahmad Safi & Hibino, 2019).

### Local Explosion Load

To get a total system solution, it is must define about the dynamic load function that acts on the system. This research uses two models of local explosion load. The description of the behavior of explosion is using an explosive load of 10 kg TNT, with a graph of the amplitude against the duration respectively with the value of  $P_{so} = 3888N$  and duration of  $t_{total} = 0.311s$ . The steps for determining the blast load parameters are as follows:

1. Determine the explosion scenario, the mass of the explosive material ( $W$ ), the distance from the center of the explosion to the structure under consideration ( $R$ ) in equation (20).

$$Z = \frac{R}{\sqrt[3]{W}} \quad (20)$$

2. Determining the part of the structure that is affected by the explosion. This study uses the part of the plate structure against the position of the explosion which is shown in Figure 4 below.

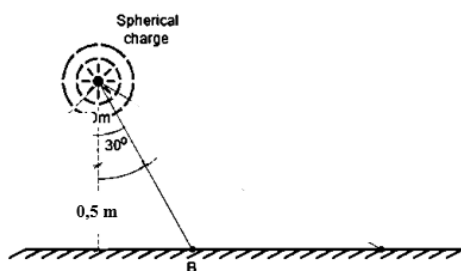


Figure 4. Distance of Explosion to the Affected Viewing Point (Karlos & Solomon, 2013)

3. Calculating the Distance Scale ( $Z$ ) using equation (20).
4. Explosion scenario using 1 variants of TNT explosion magnitude: 5 kg, using

Figure 5 to get the maximum amplitude parameter of the positive phase,  $P_{so}$  which in the polynomial equation is called  $P_{r, max}$ .

5.  $P_{r, min}$ , obtained through the 4<sup>th</sup> order polynomial equation.
6. Determining the positive phase  $t_d$  parameter using Figure 5 for the calculated  $z$  value, then the positive phase duration,  $t_0$ .
7.  $t_d^-$  negative phase is generated from the polynomial equation generated model of the 4<sup>th</sup> order.

### Numerical Results and Discussion

Numerical calculations are operated on various problem parameters with the number of modes in the  $x$  and  $y$  directions taken as  $m = 1, 2, \dots, 5$  and  $n = 1, 2, \dots, 5$  taking into account the convergence of eigenvalues. Slab parameters are plate length  $a = 8$  m, plate width  $b = 5$  m, plate thickness  $h = 0.23$  m, using a stiffener beam with a size of  $30 \times 50$  cm<sup>2</sup>, which the beam height includes the slab thickness. The density for concrete is  $2400$  kg / m<sup>3</sup>. The plate is orthotropic, so the modulus of elasticity and poisson ratio are in the  $X$  and  $Y$  directions, namely  $E_{cx} = 23400$  MPa,  $E_{cy} = 22200$  MPa (Shahsavari & Tofghi, 2014), ( $\nu_x = 0.2$  and  $\nu_y = 0.15$ ). The rotational stiffness takes a reference from Gibigaye's journal, namely  $k_1$  and  $k_2$  are equal to  $1.0 \times 10^6$  N.m / rad (Gibigaye et al., 2018).

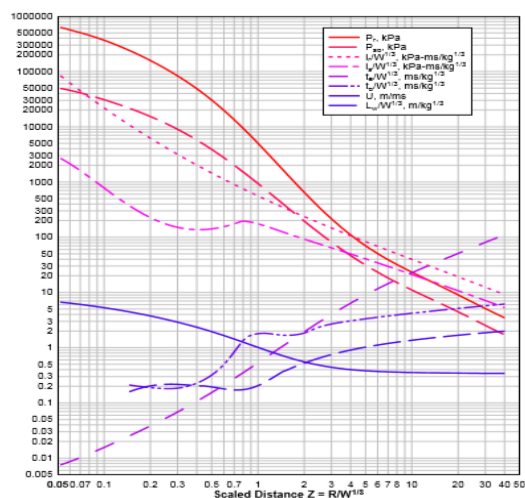


Figure 5. Positive Phase Parameters of Spherical Shock Wave for TNT in Free Air (Karlos et al., 2016)



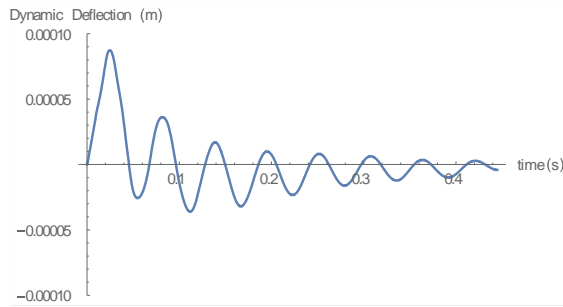


Figure 6. Time History of Explosion Phase Deflection

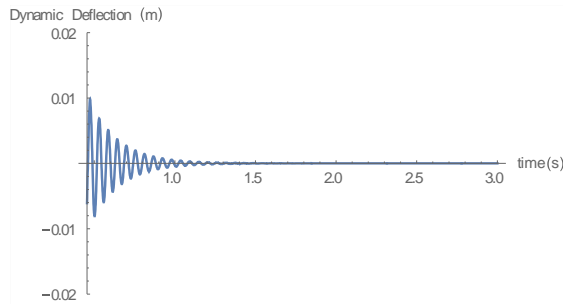


Figure 7. Time History of Free Vibration Phase Deflection

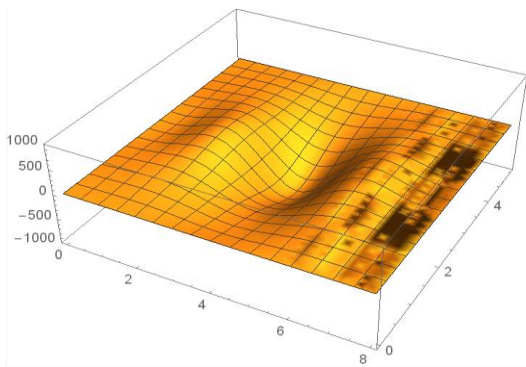


Figure 8. Maximum Deflection on the Explosive Phase

Based on SNI 2847: 2019 that the deflection requirement is  $\delta \leq \frac{l}{360}$  that  $l = 8$  m, the maximum deflection value is  $\delta = 0.022$  m (SNI 03-2847:2019, 2019). Figures 6 and 8 show that the maximum deflection that occurs is -0.013, so that it still meets the plate bending requirements due to the dynamic load of the 10 kg TNT explosion.

The deflection factor is very influential on the magnitude of the moment and the shear force that occurs on the plate. The moment and shear observed at the time of the explosion (phase 1), are the moments and shear at the maximum and minimum

conditions. The magnitude of the moment and shear obtained from the analysis results are as follows:

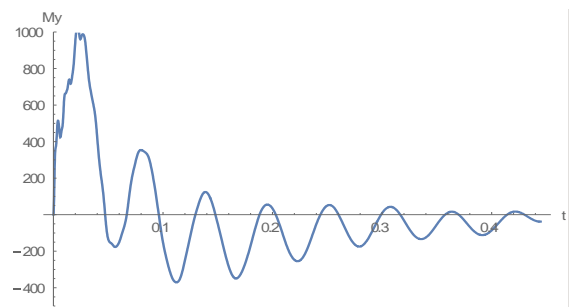


Figure 9. Time History of Moment of Y Direction

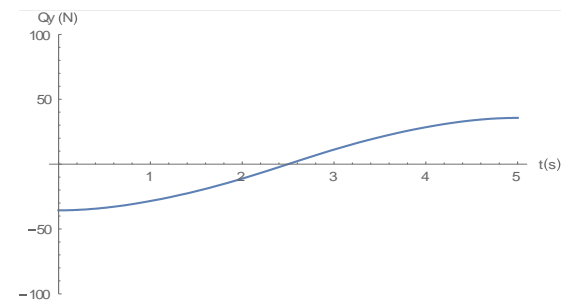


Figure 10. Shear Force on Partial Fixity

Based on those moments and shear forces, the absolute moment in the middle of the maximum span occurs in the explosion phase of 964.4 N.m which occurs on the Y axis. Meanwhile, the shear force on the support is 35.68 N.

The stress contour pattern of each load phase shows that the explosion position in the middle of the span is as Figure 11. The stress in the free vibration phase produces the largest stress, which is  $2.5 \times 10^7$  N / m<sup>2</sup>.

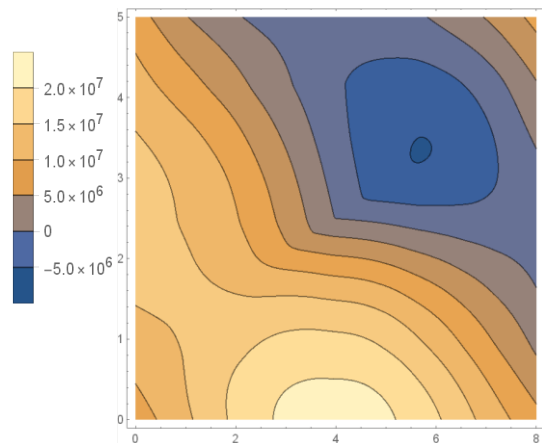


Figure 11. Maximum Stress on the Free Vibration Phase

## 2. CONCLUSION

The Reed explosion equation in 1977 at one unit condition has an error factor greater than the 4<sup>th</sup> order polynomial. Reed's modification is enhanced with the 4<sup>th</sup> order polynomial equation. The error for the Friedlander equation is 1.64%. From that statement, the dynamic behavior of orthotropic floor slabs with a thickness of 23 cm with a stiffener beam of 30x50 cm<sup>2</sup> fulfills the deflection requirements standardized by SNI 2847: 2019. The biggest deflection is on free vibration condition and it is equivalent to a moment. Different from the shear force, the moment reaches the absolute maximum is at the center of the span, while the shear is along the side of the plate with partial fixity. The absolute stress that is reviewed is the same as the moment, so that the maximum is in the middle of the span at 0.3424s

## REFERENCES

- [1] Ahmad Safi, W., & Hibino, Y. (2019). Correlation between shear and normal strength for brittle reinforced concrete member considering internal stress condition of concrete. *MATEC Web of Conferences*, 270, 01007. <https://doi.org/10.1051/mateconf/201927001007>.
- [2] Ahmet Tuğrul, & Sevim, B. (2017). Numerically and empirically determination of blasting response of a RC retaining wall under TNT explosive. *Advances in Concrete Construction*, 5(5), 493-512. <https://doi.org/10.12989/acc.2017.5.5.493>.
- [3] Bryant, L. M., Erekson, J. M., & Herrle, K. W. (2013). Are you positive about negative phase? *Structures Congress 2013: Bridging Your Passion with Your Profession - Proceedings of the 2013 Structures Congress*, 103-114. <https://doi.org/10.1061/9780784412848.010>.
- [4] Buwono, H. K., Alisjahbana, S. W., & Najid. (2020). Modification Modeling Of The Friedlander' s Blast Wave Equation Using The 6th Order Of Polynomial Equation. *International Journal of Civil Engineering and Technology (IJCIET)*, 11(2), 183-191.
- [5] Garces, M. (2019). Explosion Source Models. In *Infrasound Monitoring for Atmospheric Studies*. Springer International Publishing. <https://doi.org/10.1007/978-3-319-75140-5>.
- [6] Gibigaye, M., Yabi, C. P., & Degan, G. (2018). Free vibration analysis of dowelled rectangular isotropic thin plate on a Modified Vlasov soil type by using discrete singular convolution method. *Applied Mathematical Modelling*, 61, 618-633. <https://doi.org/10.1016/j.apm.2018.05.019>
- [7] Karlos, V., & Solomon, G. (2013). Calculation of blast loads for application to structural components. In *Publications Office of the European Union*. <https://doi.org/10.2788/61866>.
- [8] Karlos, V., Solomos, G., & Larcher, M. (2016). Analysis of the blast wave decay coefficient using the Kingery- Bulmash data. *International Journal of Protective Structures*, 7(3), 409-429. <https://doi.org/10.1177/2041419616659572>.
- [9] Pevzner, P., Weller, T., & Berkovits, A. (2000). Further modification of Bolotin method in vibration analysis of rectangular plates. *AIAA Journal*, 38(9), 1725-1729. <https://doi.org/10.2514/2.1159>
- [10] Rigby, S. E., Tyas, A., Bennett, T., Clarke, S. D., & Fay, S. D. (2014). The negative phase of the blast load. *International Journal of Protective Structures*, 5(1), 1-19. <https://doi.org/10.1260/2041-4196.5.1.1>.

- [11] Shabana, A. A. (2014). Theory of vibration - An introduction. In *Katalog BPS: Vol. XXXIII* (Issue 2). <https://doi.org/10.1007/s13398-014-0173-7.2>.
- [12] Shahsavar, V. L., & Tofighi, S. (2014). Uncertainties Concerning the Free Vibration of Inhomogeneous Orthotropic Reinforced Concrete Plates. *Slovak Journal of Civil Engineering*, 22(3), 21–30. <https://doi.org/10.2478/sjce-2014-0014>.
- [13] Smyth, B. G. K. (2014). Polynomial approximation. *North-Holland Mathematics Studies*, 11(C), 67–75. [https://doi.org/10.1016/S0304-0208\(08\)71986-8](https://doi.org/10.1016/S0304-0208(08)71986-8).
- [14] SNI 03-2847:2019. (2019). SNI 03-2847:2019 Persyaratan Beton Struktural Untuk Bangunan Gedung Dan Penjelasan Sebagai Revisi Dari Standar Nasional Indonesia 2847 : 2013. *Badan Standarisasi Nasional*, 03-2847:20(8), 1–695



